Process Design of Onboard Membrane Carbon Capture and Liquefaction Systems for LNG-Fueled Ships

Juyoung Oh[a], Rahul Anantharaman[b], Umer Zahid[c], PyungSoo Lee[d,*], Youngsub Lim[a,*]

[a] Department of Naval Architecture and Ocean Engineering, Seoul National University, 1 Gwanak-ro, Gwanak-gu, Seoul, 08826, Republic of Korea

[b] SINTEF Energy Research, NO-7465 Trondheim, Norway

[c] Chemical Engineering Department, King Fahd University of Petroleum & Minerals (KFUPM), Dhahran 31261, The Kingdom of Saudi Arabia

[d] Department of Chemical Engineering and Material Science, Chung-Ang University, 84 Heukseok-ro, Dongjak-gu, Seoul, 06974, Republic of Korea

[*] Corresponding author

E-mail address: leeps@cau.ac.kr (PyungSoo Lee), s98thesb@snu.ac.kr (Youngsub Lim)

Abstract

This study proposes an onboard membrane carbon capture and liquefaction system for LNG-fueled ships to satisfy the IMO's 2050 greenhouse gas reduction targets. The exhaust gas from a natural gas ship has a low CO_2 fraction (~3%) and high O_2 fraction (~16%) compared to the flue gas from power plants. Herein, considering the above distinguishing features, a membrane carbon capture and liquefaction system has been proposed that is energy efficient and compact for the application of ships. To ascertain the performance of the proposed membrane-based system, it is compared to an amine-based onboard system in terms of energy consumption and major equipment size. This work evaluates four process configurations by varying the number of membrane stages and associated liquefaction processes at different CO_2/N_2 selectivity and CO_2 permeance. The results show that energy consumption (3.98 GJ_e/t_{LCO2}) is higher than the amine-based system (3.07 GJ_e/t_{LCO2}) at the CO_2/N_2 selectivity of 50, but it can be decreased to 3.14 and 2.82 (GJ_e/t_{LCO2}) with improved selectivity of 100 and 150, respectively. The major equipment size decreases to 54%, 28%, and 20% of the amine-based system when the permeance is 1000, 2000, and 3000 GPU, respectively. The results indicate that the new onboard membrane carbon capture and liquefaction system can be a competitive solution for the IMO's greenhouse gas reduction targets for 2050.

Keywords

Onboard CCS; Membrane CO_2 separation; CO_2 Liquefaction; Process Design; Ship-based exhaust gas

Nomenclature

A_m	membrane area [cm^2]
L_f	feed flow rate [Scm^3/s]
MDO_f	MDO mass flow rate [kg/h]
P_1	compression pressure at stage 1 [bar]
P_2	compression pressure at stage 2 [bar]
P_3	compression pressure at stage 3 [bar]
P_4	compression pressure at stage 4 [bar]
P'_A	permeability of component A [$Scm^3 \cdot cm \,/\, (s \cdot cm^2 \cdot cmHg)$]
p_h	feed pressure [cmHg]
p_l	permeate pressure [cmHg]
R_1	Recycle ratio at 1st membrane [%]
R_2	Recycle ratio at 2nd membrane [%]
R_3	Recycle ratio at liquefaction [%]
t	membrane thickness [cm]
T_1	Temperature before the J-T valve 1 [°C]
T_2	Temperature before the J-T valve 2 [°C]
V_p	permeate flow rate [Scm^3/s]
x_{fi}	mole fraction of component *i* on the feed side [mol%]
y_1	mole fraction of permeate 1 stream [mol%]

y_2	mole fraction of permeate 1 stream [mol%]
y_{pi}	permeate mole fraction of component i [mol%]
$\alpha_{A/B}$	A/B selectivity [-]
θ	membrane stage cut [-]
θ_1	membrane 1 stage cut [%]
θ_2	membrane 2 stage cut [%]
η_b	thermal efficiency of the boiler [%]
BSGC	Brake specific exhaust gas flow
BSPC	Brake specific gas consumption
CCS	Carbon capture and storage
DWT	Deadweight
EEDI	Energy efficiency design index
GHG	Greenhouse gas
IMO	International maritime organization
LCC	Life cycle cost
LCO_2	Liquefied CO_2
LHV	Lower heating value

LNG	Liquefied natural gas
MCR	Maximum continuous rating
MDEA	Methyldiethanolamine
MDO	Marine diesel oil
MEA	Monoethanolamine
MEPC	Marine environment protection committee
OCCS	Onboard carbon capture and storage
PZ	Piperazine
SEC	Specific energy consumption
SFOC	Specific fuel oil consumption
SQP	Sequential quadratic programming
TEU	Twenty-foot equivalent unit
TPD	Ton per day

1. Introduction

As drastic climate change caused by global warming has emerged as a major environmental issue, the energy efficiency design index (EEDI), which measures in grams of CO_2 emissions generated by a ship to transport 1 ton of cargo per 1 nautical mile, was adopted by the International Maritime Organization (IMO) as a mandatory measure to reduce greenhouse gas (GHG) emissions from international shipping. According to the fourth IMO GHG study, GHG emissions caused by international shipping increased to 2.89% of the total global GHG emissions in 2018 [1]. The IMO Marine Environment Protection Committee (MEPC) during their 74th proceeding agreed on further strengthening the Phase 3 EEDI requirements. This includes the EEDI reduction rates for container ships up to 50% and accelerated implementation of schedules for some ship types starting 2022 [2,3]. In addition, the EEDI Phase 4 was considered, and the IMO GHG strategy is to reduce EEDI by a minimum of 40% and 70% by 2030 and 2050, respectively [4].

The IMO's plan of decreasing EEDI up to 70% now engenders the introduction of carbon capture and storage (CCS) technologies onboard. The IMO's EEDI Phase 3 requirements can be achieved by using LNG fuel, combined with existing technologies such as hull form optimization, voyage optimization, and speed reduction [5]. This means that its EEDI value is lower than the EEDI Phase 3 value. To meet the IMO's 2050 target of reducing EEDI up to 70%, alternative low and zero carbon fuels, such as hydrogen, need to be considered [6,7]. However, various limitations such as fuel supply for shipping, safety concerns, and low energy density are key hurdles in making near future implementation infeasible. Therefore, to meet the IMO's 2050 target, proven technologies that can be applied to ships must be considered. CCS technology is a proven technology for onshore power plants and can be applied to ships for onboard carbon capture and storage (OCCS) systems [8–13]. CCS technology works by

capturing CO_2 from the ship's engine exhaust gas, storing the captured CO_2, and unloading the captured CO_2 to the safe storage sites.

Currently, a chemical absorption process using amines is the most commonly proposed carbon capture process in OCCS systems. Lee et al. [9] presented an EEDI estimation method reflecting an OCCS system based on chemical absorption with an activated methyldiethanolamine (MDEA). Feenstra et al. [10] suggested a chemical absorption process for carbon capture on diesel and LNG-fueled ships by using MEA and piperazine (PZ) as solvents and conducted techno-economic evaluations. Van den Akker [12] investigated the feasibility of carbon capture using MEA solvent on LNG-fueled ships in terms of energy and economic feasibility. However, the solvent-based chemical absorption process requires significant space for equipment of the absorber and the stripper. This is an obvious limitation for an onboard system with limited space. For example, an 8000 DWT general cargo ship with a 7.3 m draft, one of the main dimensions of ships, requires 10 m and 14 m height of the absorber and stripper, respectively [12]. This process, which requires two tall columns, can encounter the economic loss resulting from the cargo loss. Therefore, the size of the OCCS system is an important factor that must be considered while selecting the onboard carbon capture system to minimize the cargo loss of ships because of system installation.

Another carbon capture technology, a membrane capture process, requires much smaller space than the absorption process [14]. Therefore, it is a practical alternative solution for the application to an onboard system with limited space. Merkel et al. [15] reported that only a 12 ft wide × 47 ft long × 23 ft tall pilot membrane system was required to treat coal-derived flue gas containing 20 tons CO_2/day (20 TPD), while a solvent capture system for a 10 TPD scale required a 150 ft tall column. Zhao et al. [16] conducted a parametric study for multi-stage membrane systems that assumed a binary mixture (14 mol% CO_2 and 86 mol% N_2) based on a

coal-fired power plant. Hussain et al. [17] performed a feasibility study of carbon capture for low CO_2 mole fraction (10%) using a membrane with the facilitated transport mechanism to investigate energy consumption and processing cost. Merkel et al. [18] reported process sensitivity studies for estimating energy consumption, membrane area, and cost by varying a stage of the membrane process, flow pattern, and membrane performance based on a coal-fired power plant. Ramasubramanian et al. [19] investigated a cost analysis of a multi-stage air-sweep process according to the membrane performance and feed CO_2 mole fraction. Xu et al. [20] carried out a membrane gas separation process for a multicomponent mixture to optimize its space requirements and energy efficiency with flue gas having 68.8% N_2, 13.5% CO_2, 15.3% H_2O, and 2.4% O_2. Micari et al. [18] explored the techno-economic assessment of post-combustion carbon capture using nanoporous single-layer graphene membranes. Evaluations were performed for two flue gas scenarios: one was the case of dry feed with 10% CO_2 and 90% N_2 and the other was the case of wet feed containing 10% CO_2, 15% H_2O, 3% O_2, and 72% N_2. Most of the above-mentioned previous studies focusing on membrane carbon capture processes were based on coal-based power plants where the mole fraction of CO_2 in the flue gas is relatively high. However, the exhaust gas from the LNG-fueled ship has a very low CO_2 mole fraction (~3%) and a high O_2 mole fraction (~16%) [9]. These features can severely affect the performance of the membrane; therefore, a suitable composition and model should be studied to appropriately evaluate the membrane capture process for an OCCS system.

This study aims to propose a competitive new OCCS system, an onboard membrane carbon capture and liquefaction system, considering a ternary mixture of N_2, O_2, and low mole fraction CO_2. Membrane carbon capture systems were designed to satisfy the IMO's greenhouse gas reduction targets for 2050, and the energy consumption of each case was evaluated with various membrane performances. The results were compared with the amine-based capture process in terms of energy consumption and major equipment size.

2. Background

2.1 Mathematical model of membrane process

Several ideal flow patterns have been suggested for membrane gas separation [19]. It has been reported that the complete mixing (perfect mixing) flow pattern has a conservative separation performance compared to cross-flow, co-current, and countercurrent flows [20], which means that it is appropriate for a conservative design approach. Figure 1 shows a complete mixing pattern that assumes no concentration gradient according to the direction of the gas flow on the low-pressure side (permeate side) and the high-pressure side (feed side), and the main assumptions of the membrane model are [22]:

- Membrane models for gas separation are isothermal conditions.
- Pressure drop on the permeate side and the feed side are negligible.
- The permeability of each component is independent of pressure.

A mathematical model of complete mixing was derived by Weller and Steiner [21].

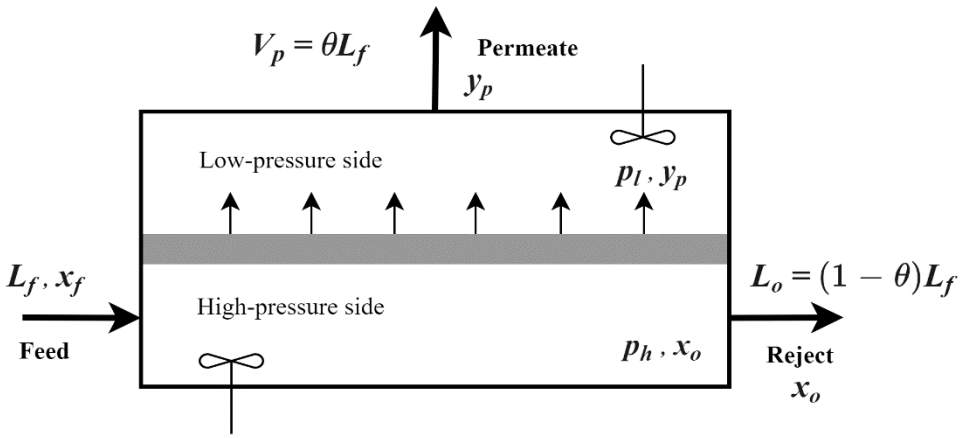

Figure 1. Process flow for complete mixing model

174

175 The membrane stage cut θ is defined as:

$$\theta = \frac{V_p}{L_f} \quad (1)$$

176 where L_f and V_p are the feed flow rate and permeate flow rate (Scm^3/s), respectively.

177 For a binary mixture (components A and B), the permeate mole fraction y_{pA} was calculated
178 using Eq. (2) [19].

179

$$y_p = \frac{-b + \sqrt{b^2 - 4ac}}{2a} \quad (2)$$

180 where,

181 $$a = \theta + \frac{p_l}{p_h} - \frac{p_l}{p_h}\theta - \alpha\theta - \alpha\frac{p_l}{p_h} + \alpha\frac{p_l}{p_h}\theta$$

182 $$b = 1 - \theta - x_f - \frac{p_l}{p_h} + \frac{p_l}{p_h}\theta + \alpha\theta + \alpha\frac{p_l}{p_h} - \alpha\frac{p_l}{p_h}\theta + \alpha x_f$$

183 $$c = -\alpha x_f$$

184

185 where x_f is the mole fraction of component A on the feed side, p_h is the feed pressure
186 (cmHg), p_l is the permeate pressure (cmHg), and $\alpha_{A/B}$ is the A/B selectivity. Eq. (2) is a
187 simple function of the membrane stage cut when the membrane performance parameters
188 (selectivity or permeance) and pressure ratio are determined. The membrane area based on the
189 binary mixture is described as:

190

$$A_m = \frac{\theta L_f y_p}{(P'_A / t)(p_h x_0 - p_l y_p)} \quad (3)$$

191 $$x_o = \frac{x_f - \theta y_p}{1 - \theta}$$

192

193 where t is the membrane thickness (cm), and P'_A is the permeability of A in the membrane,
194 $\mathrm{S\,cm^3 \cdot cm\,/\,(s \cdot cm^2 \cdot cmHg)}$. For a complete mixing model of a ternary mixture, the
195 permeate mole fraction of component i, y_{pi}, is described by Eq. (4) [19].

196

$$y_{pi} = \frac{p_h x_{fi}/(1-\theta)}{(V_P t/(P'_i A_m) + \theta p_h/(1-\theta) + p_l)} \quad (4)$$

197

198 where x_{fi} is the mole fraction of component i on the feed side and the membrane area, A_m,
199 is calculated using Eq. (5).

200

$$A_m = \frac{V_p y_{pi} t}{P'_i[\frac{p_h(x_{fi} - \theta y_{pi})}{(1-\theta)} - p_l y_{pi}]} \quad (5)$$

201

202 Figure 2 shows the numerical procedure to calculate y_{pi}.

203

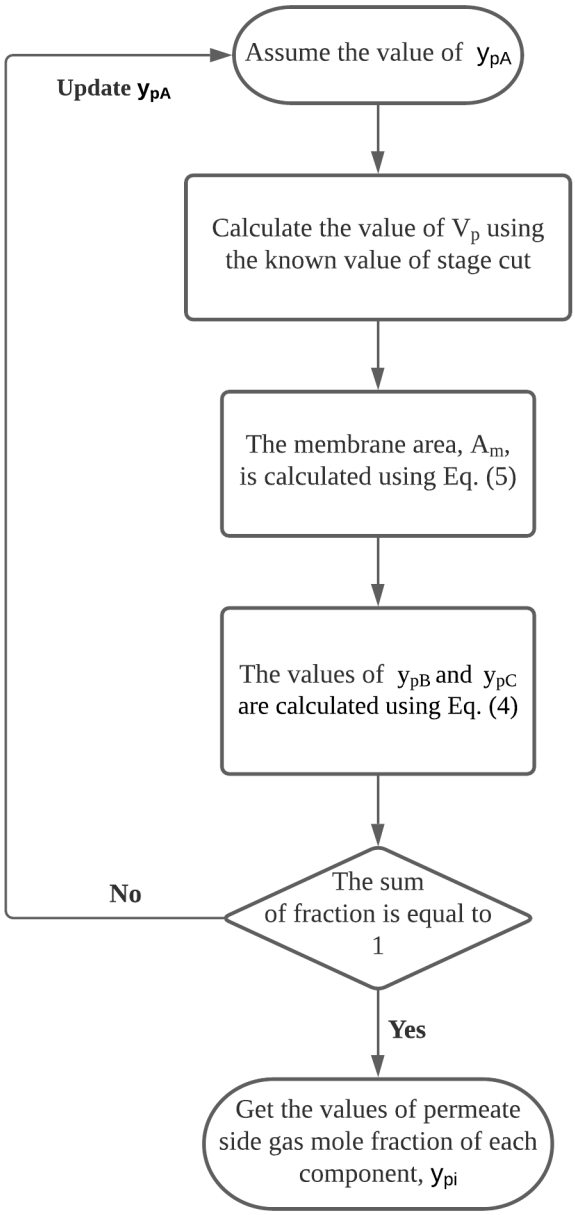

204

205 Figure 2. Procedure for the calculation of the permeate side gas mole fraction for a ternary

206 mixture.

207

208 **2.2 CO_2 liquefaction process**

209 When the captured CO_2 is transported by a ship, liquefied CO_2 (LCO_2) is recommended

210 because of the amount of CO_2 emissions from the ship's engine and the volume of the storage

tank [22]. That is, if the captured CO_2 is transported as gaseous CO_2, its volume is approximately 500 times larger than that of LCO_2 [23]. The triple point of CO_2 is 5.18 bar and -56.57 °C; therefore, a storage pressure higher than 5.18 bar is required for liquid storage. Previous studies proposed a storage pressure of 6.5–20 bar [24–27], and Seo et al. [28] proposed that 15 bar is an appropriate pressure considering the life cycle cost (LCC) of ship-based carbon capture and storage chains.

For liquefaction of CO_2, various processes have been studied [29,30]. Seo et al. [23] investigated four prominent liquefaction systems and concluded that a pre-cooled Linde-Hampson system showed high performance. Based on the results reported in the above literature, this work assumed the pre-cooled Linde-Hampson system for the liquefaction of onboard captured CO_2.

2.3 Reference amine-based OCCS systems (Case 1)

Lee et al. [9] researched an amine-based OCCS system targeting an EEDI 70% reduction. The CO_2 from the natural gas ship engine was captured using an activated MDEA solution, and the captured CO_2 was liquefied through the liquefaction process using LNG and ammonia. They reported the energy consumption and sizing results, as shown in Table 1. To compare the membrane onboard system with the amine-based onboard system, this previous study was defined as a reference case, Case 1.

Table. 1. Simulation results of an amine-based OCCS system [9]

Category	Unit	Value
Target ship		3800 TEU container

EEDI reduction rate	%	70
Capture SEC_{th}	GJ_{th}/t_{CO2}	3.30
Additional power for capture process	kWh/t_{CO2}	54.9
Liquefaction SEC	kWh/t_{CO2}	98.0
Captured CO_2 flow rate	ton/h	3.651
CO_2 mole fraction	%	2.79
Absorber diameter	m	3.1
Absorber packing height	m	7
Absorber total height	m	13.5
Stripper packing diameter	m	1.2
Stripper sump diameter	m	3.1
Stripper packing height	m	3.25
Stripper total height	m	10

To fairly compare the energy consumption for each OCCS system, the specific energy consumption (SEC) of thermal energy (GJ_{th}) for the solvent regeneration of Case 1 was converted to equivalent electric energy consumption (GJ_e) based on the consumption of marine diesel oil (MDO). The assumptions of the lower heating value (LHV) of the MDO, the thermal efficiency of the boiler (η_b), and the specific fuel oil consumption (SFOC) of the generator are listed in Table. 2. Firstly, the MDO mass flow rate (MDO_f) required to generate the required equivalent thermal energy for the solvent regeneration of Case 1 (3.30 GJ_{th}/t_{CO2}) was calculated using Eq. (6).

$$MDO_f\ [\text{ton/h}] = (Total\ heat\ duty)\left(\frac{1}{(LHV_{MDO})(\eta_b)}\right) \quad (6)$$

$$Total\ heat\ duty\ [GJ_{th}/h] = (\ Capture\ SEC\ [GJ_{th}/t_{co2}])(Captured\ CO_2\ flow\ rate\ [\text{ton/h}])$$

$$\frac{1}{(LHV_{MDO})(\eta_b)}\ [\mathrm{GJ/ton}] = \textit{Required MDO mass flow rate to generate } 1\ \mathrm{GJ_{th}}$$

Secondly, the electric energy consumption, which equivalently consumed the MDO_f, was calculated with consideration for the SFOC of the generator, as shown in Eq. (7) and Eq. (8).

$$(\textit{Electric energy consumption}\ [\mathrm{GJ}_e/\mathrm{t}_{co2}])(\textit{Captured } CO_2 \textit{ flow rate}\ [\mathrm{ton/h}]) = \frac{MDO_f\ [\mathrm{ton/h}]}{(SFOC\ [\mathrm{ton/GJ}])} \quad (7)$$

Finally, Eq. (7) was rearranged to calculate the equivalent electric energy consumption.

$$\textit{Electric energy consumption}\ [\mathrm{GJ}_e/\mathrm{t}_{co2}](=\textit{Amine regeneration}) = \frac{MDO_f\ [\mathrm{ton/h}]}{(SFOC\ [\mathrm{ton/GJ}])(\textit{Captured } CO_2 \textit{ flow rate}\ [\mathrm{ton/h}])} \quad (8)$$

The required major equipment size for Case 1 was estimated from the reported sizing results of the absorber, stripper and sump tank from Table 1.

Table. 2. Assumption for energy unit conversion

Category	Unit	Value
LHV_{MDO}	GJ/ton	42.7 [31]
Boiler efficiency (η_b)	%	65 [35,36]

SFOC of generator	ton/GJ	0.047[*1]

[*1] The SFOC of the generator was estimated by 5X35-B diesel engine data from WinGD GTD.

Table 3 shows the conversion of thermal energy to electric energy results, with consideration of Table 2 and the sizing results of Case 1.

Table. 3. Energy and sizing results of Case 1

Category		Unit	Value
Capture	Amine regeneration	GJ_e/t_{CO2}	2.52[*1]
	Others		0.198 [9]
Liquefaction	Compression		0.35 [9]
LCO_2		ton/h	3.651 [9]
Total SEC		GJ_e/t_{LCO2}	3.07
Main equipment size		m^3	177.37 [9][*2]

[*1] converted by Eq. (8).

[*2] estimated by the reported sizing results of the absorber, stripper, and sump tank.

3. Modeling and Simulation

This study defined three major cases.

1. Case 1 was a reference case based on an amine solvent capture process combined with a liquefaction process.
2. Case 2 was a membrane capture process combined with a liquefaction process, and the exhaust gas was assumed to be a binary mixture of N_2 and CO_2; this is not a practical composition, but was studied to show the effect of O_2 existence in the practical exhaust gas.
3. Case 3 was a membrane capture and liquefaction process, but considered a ternary mixture of N_2, O_2 and CO_2.

Cases 2 and 3 studied four different configurations considering the number of stages for the membrane and the liquefaction processes. M1 and M2 represent the single-stage and two-stage membrane processes, respectively. L1 and L2 represent the single-stage and two-stage cascade liquefaction processes, respectively.

Figure 3 shows the four process configurations of M1-L1, M1-L2, M2-L1, and M2-L2 used for Case 3. For the membrane process, a mathematical model of complete mixing membrane for a ternary mixture were built based on a previous study [19]. It was coded in a process simulation software, Aspen HYSYS V10, as a spreadsheet and combined with a splitter module. For property calculation, the Peng-Robinson equation of state was used. One stage (M1) and two stages (M2) of the membrane process were considered. Recycling a reject stream to the inlet stream of the membrane may help increase the resulting target material mole fraction of the permeate stream. Therefore, two decision points of R1 and R2 were added to evaluate the effect of recycling reject streams. The captured CO_2 from the membrane process is liquefied

through the liquefaction process. For the single-stage liquefaction process (L1), a propene refrigeration cycle was modeled. When the CO_2 inlet mole fraction is low, the required temperature for CO_2 separation becomes lower because of the high N_2 and O_2 contents, so the single-stage liquefaction is not enough; therefore, an ethane-propene cascade cycle (L2) was modeled. After JT expansion, most nitrogen and oxygen contents are removed as vapor, and high mole fraction LCO_2 is generated. The vapor stream is still low temperature, so it is used to cool down the inlet stream by heat exchange. The vapor stream still contains some portion of CO_2, so partial or full recycling of the vapor stream to the inlet stream to the liquefaction process may increase the liquefaction efficiency. R3 is used to evaluate the effect of no/partial/full recycling of the vapor stream. For Case 2, a mathematical model of complete mixing membrane for a binary mixture was built and combined with Aspen HYSYS. The process scheme is similar to Case 3, but only the single-stage liquefaction process (L1) was considered for Case 2 because this considered only a binary mixture of N_2 and CO_2, resulting in high mole fraction CO_2 being captured from the membrane process. Table 4 shows the assumptions for the membrane and liquefaction processes.

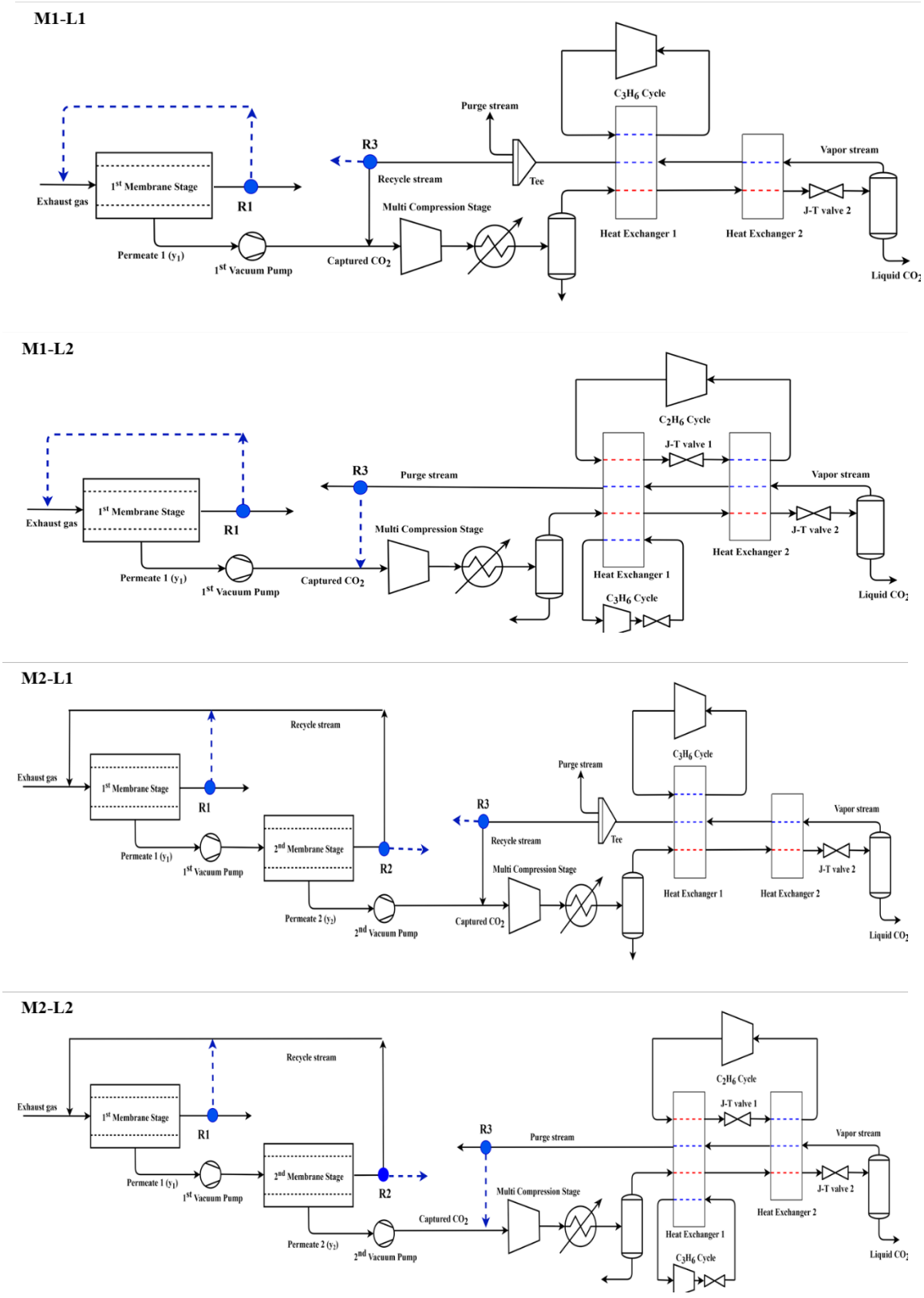

Figure 3. Process flow diagram of the four configurations

315 Table. 4. Assumptions for the capture and liquefaction process simulation

Category	Unit	Value
Membrane process		
Flow pattern		Complete mixing
Feed pressure	bar	1.05
Vacuum pump efficiency (adiabatic)	%	85 [33]
Vacuum level (pressure ratio)		20
Membrane CO_2/N_2 selectivity		50 [15]
Membrane O_2/N_2 selectivity		5 [34,35]
Membrane CO_2 permeance	GPU	1000 [15]
Thickness	cm	10^{-5} [15]
Liquefaction process		
Compressor efficiency (adiabatic)	%	75
Storage pressure	bar	15 [28]
Cooling water temperature	℃	30
Minimum temperature at coolers	℃	5 [23]
Pressure drop	bar	0 [36]
Refrigerant for single liquefaction		Propene
Refrigerants for cascade liquefaction		Propene and Ethane

316

317 **3.1 Target ship and exhaust gas condition**

318 In this study, a 3800 TEU container feeder fueled by LNG was selected as the target ship [9].
319 The main specifications are listed in Table 5.

320

321 Table. 5. Main specifications of target ship [37]

Category	Unit	Value
Length over all	m	224.8
Breadth	m	37.50
Depth	m	19.10
Draft, scantling	m	12.50
Deadweight	DWT	53,200
$MCR_{Main\ engine}$	kW	18,200
Reference speed	knots	17[*1]

[*1] The reference speed was estimated using the Korean Register (KR) GEARs program.

To design an appropriate capture system, the composition of the feed gas was estimated using the General Technical Data (GTD) application of WinGD, which provided the performance data of the main engine, as shown in Table 6.

Table. 6. Performance data of main engine from GTD

Category	Unit	Value
Power	%	75
	kW	13,650
BSGC	g/kWh	140.8
	kg/h	1,921
BSPC	g/kWh	1
	kg/h	13.65
Scavenge air	kg/h	122,323

329

330 Considering the performance data from the main engine of the LNG-fueled ship, the
331 composition of the exhaust gas was calculated, and it was assumed that the other components
332 of the exhaust gas, such as water, NO_X, and SO_X were removed, as shown in Table 7. Case 2
333 did not consider the presence of oxygen in the exhaust gas contrary to the Case 3.

334

335 Table. 7. Estimated exhaust gas condition of the target ship

Case	Components	Mole fraction [%]
Case 1: Reference case [9]	CO_2	2.79
	N_2	75.31
	O_2	14.81
	H_2O	6.19
	Ar	0.9
Case 2: Binary mixture case	CO_2	2.94
	N_2	97.06
Case 3: Ternary mixture case	CO_2	2.94
	N_2	81.39
	O_2	15.67

336

337 **3.2 Required CO_2 reduction**

338 In order to achieve the desired EEDI level, a proportionate level of CO_2 reduction is required.
339 It was assumed that the CO_2 reduction of the OCCS system was reflected in the carbon
340 reduction technology term of the EEDI formula [1]. The calculated EEDI values are shown in

Table 8, which shows that the EEDI of the target ship using LNG fuel can satisfy the target of an EEDI 35% reduction in 2022, but cannot satisfy the IMO's 2050 target of EEDI 70% reduction. To satisfy this requirement, an additional 2074 kg/h CO_2 reduction from the exhaust gas is required.

Table. 8. Calculated EEDI and CO_2 reduction of the target ship.

Attained EEDI	
EEDI of the target ship	9.1412
Required EEDI	
2022 EEDI target (35% reduction)	12.7088
2050 EEDI target (70% reduction)	5.8656
Required CO_2 reduction rate	2074 kg/h

3.3 Process optimization and major equipment sizing

Energy consumption is a crucial factor in determining the feasibility of an OCCS system. In this study, the energy consumption consisted of two major parts: the energy consumed by the vacuum pump in the membrane capture process, and the compressors in the liquefaction process. There is a trade-off between energy consumption in the capture and liquefaction processes. If the number of membrane stages increases, the resulting mole fraction of the captured CO_2 increases leading to a reduced liquefaction energy.

Therefore, to minimize the total energy consumption required per ton of LCO_2, the process was optimized using the Aspen HYSYS sequential quadratic programming (SQP) optimizer

with fixed membrane selectivity and permeance. The optimization variables and constraints are listed in Table 9.

Table. 9. Optimization variables and constraints of energy consumption

Variables	Unit	Process
θ_1 (Membrane 1 stage cut)		Capture
θ_2 (Membrane 2 Stage cut)		Capture
R_1 (Recycle ratio at 1st membrane)		Capture
R_2 (Recycle ratio at 2nd membrane)		Capture
P_1 (Compression pressure at stage 1)	bar	Liquefaction
P_2 (Compression pressure at stage 2)	bar	Liquefaction
P_3 (Compression pressure at stage 3)	bar	Liquefaction
P_4 (Compression pressure at stage 4)	bar	Liquefaction
T_1 (Temperature before the J-T valve 1)	°C	Liquefaction
T_2 (Temperature before the J-T valve 2)	°C	Liquefaction
R_3 (Recycle ratio)		Liquefaction
Constraints	**Unit**	**Value**
Compression ratio at each stage		≤4 [38]
Minimum approach temperature at heat exchangers	°C	≥3 [23]
Required CO_2 reduction	kg/h	2074

The compact system size is a dominant factor for introducing the OCCS system [39]. The membrane area required for each system was calculated using Eq. (3) for the binary mixture and Eq. (5) for the ternary mixture by varying the CO_2 permeance to 1000, 2000, and 3000

GPU with a fixed CO_2/N_2 selectivity. After the required membrane area was obtained, the volume of the membrane system for carbon capture was estimated using specific membrane module designs based on a previous study; which reported that a 5 m^3 volume of membrane module (1 m height × 1 m width × 5 m length) contains a membrane area of 2,500 m^2 [15].

4. Results and discussion

4.1 Case 2: membrane process with a binary mixture (CO_2 and N_2)

Table 10 provides the optimized process variables and simulation results of Case 2: membrane capture and liquefaction process for a binary CO_2-N_2 exhaust gas with three different selectivity 50, 100, and 150. The total SEC may not be the sum of the liquefaction SEC and the capture SEC because of the different unit. The total SEC and the liquefaction SEC are defined as the energy consumption required per ton of LCO_2, and the capture SEC is defined as the energy consumption required per ton of CO_2 captured. The results show that there is zero recycling at R1 of M1-L1 and M2-L1, and this is because the CO_2 fraction in the reject stream of the 1st membrane stage is lower than the CO_2 fraction in the exhaust gas. This means that recycling through R1 decreases the CO_2 mole fraction of permeate 1 stream. At R2, however, 100% recycling was selected because the reject stream of the 2nd membrane stage had sufficient CO_2 mole fraction to contribute to the higher CO_2 mole fraction of permeate 2 stream.

406 Table. 10. Simulation results of Case 2: binary mixture

α	Configuration	θ_1 / θ_2	y_1/y_2	R1/R2/R3	P_4	T_2	SEC [GJ_e/t_{CO2}]		
		[%]	[mol%]	[%]	[bar]	[°C]	Capture	Liquefaction	Total
50	M1-L1	5.87	22.81	0/-/39	175	-68	1.414	3.571	5.232
		/-	/-						
	M2-L1	7.27	22.76	0/100/51	144	-49	2.375	1.083	3.729
		/23.16	/71.42						
100	M1-L1	5.23	26.27	0/-/42	170	-65	1.222	3.268	4.740
		/-	/-						
	M2-L1	5.79	27.48	0/100/55	67	-46	1.928	0.840	2.916
		/23.87	/85.13						
150	M1-L1	4.96	27.88	0/-/44	170	-63	1.149	3.132	4.523
		/-	/-						
	M2-L1	5.11	29.58	0/100/48	67	-46	1.730	0.766	2.611
		/25.98	/88.30						

407

408 The results show that the two-stage membrane process (M2-L1) has a lower total energy
409 consumption compared to the single-stage membrane process (M1-L1) at all the selectivities.
410 Although Case 2-M2-L1 required more energy for capture, a high mole fraction of captured
411 CO_2 was obtained; therefore, the required energy consumption of the liquefaction process was
412 effectively decreased. Figure 4 shows the energy consumption of Case 2 processes compared
413 to that of the Case 1: the reference amine-based case. When the selectivity of the membrane
414 was 50, the energy consumption of Case 2 was higher than that of Case 1. However, when the
415 selectivity was higher than 100, the M2-L1 process showed lower energy consumption than
416 Case 1.

417

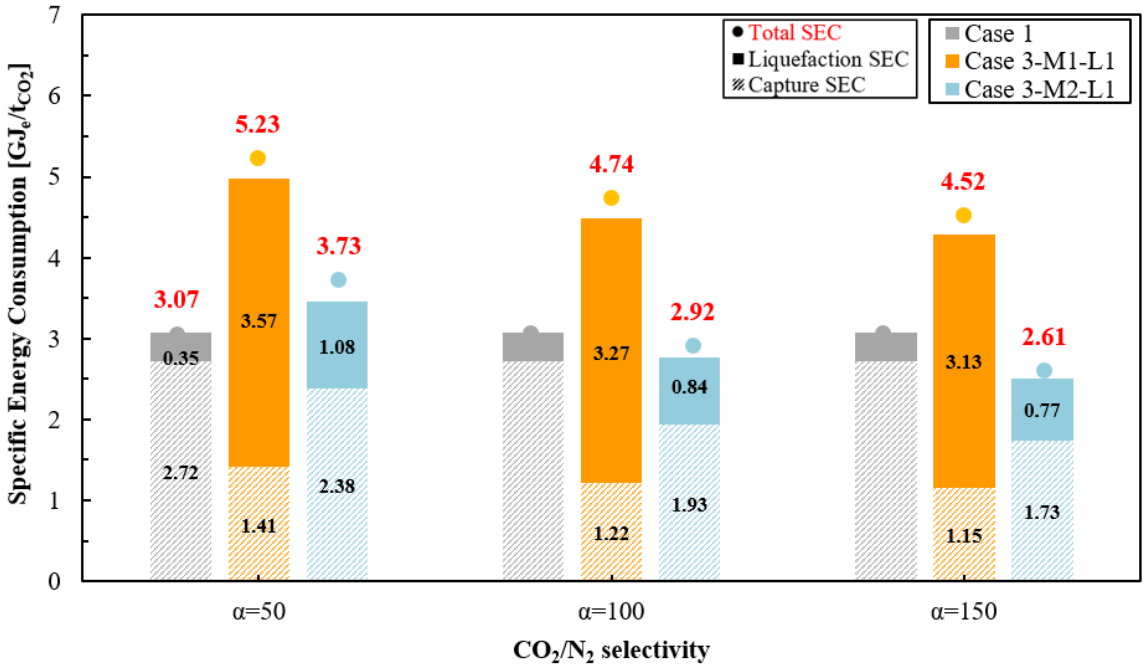

Figure 4. Total SEC and capture SEC of Case 2: membrane capture and liquefaction for the CO_2-N_2 binary mixture

The required membrane area and the number of membrane modules of Case 2 for estimating the major equipment size were summarized in Table 11. Figure 5 shows that the required major equipment size for Case 1 and Case 2 at varying permeabilities. It was observed that for Case 2, both M1-L1 and M2-L2 had smaller sizes in all CO_2 permeance except for M2-L1 of 1000 GPU, when compared to Case 1: reference amine-based case, even with the selectivity of 50. The results reveal that the membrane module volume of both designs is decreased by increasing CO_2 permeance from 1000 GPU to 3000 GPU.

Table. 11. Results of required membrane area of Case 2: binary mixture

Permeance [GPU]	Configuration	Membrane area [m^2]	Number of membrane modules[*1]	Major equipment size[*2] (Modules volume) [m^3]
1000	M1-L1	78,070	32	160
	M2-L1	111,653	45	225
2000	M1-L1	39,035	16	80
	M2-L1	55,827	23	115
3000	M1-L1	26,024	11	55
	M2-L1	37,218	15	75

[*1] rounding up the number of membrane modules to the nearest one.

[*2] estimated by a 5 m^3 volume of MTR's membrane module.

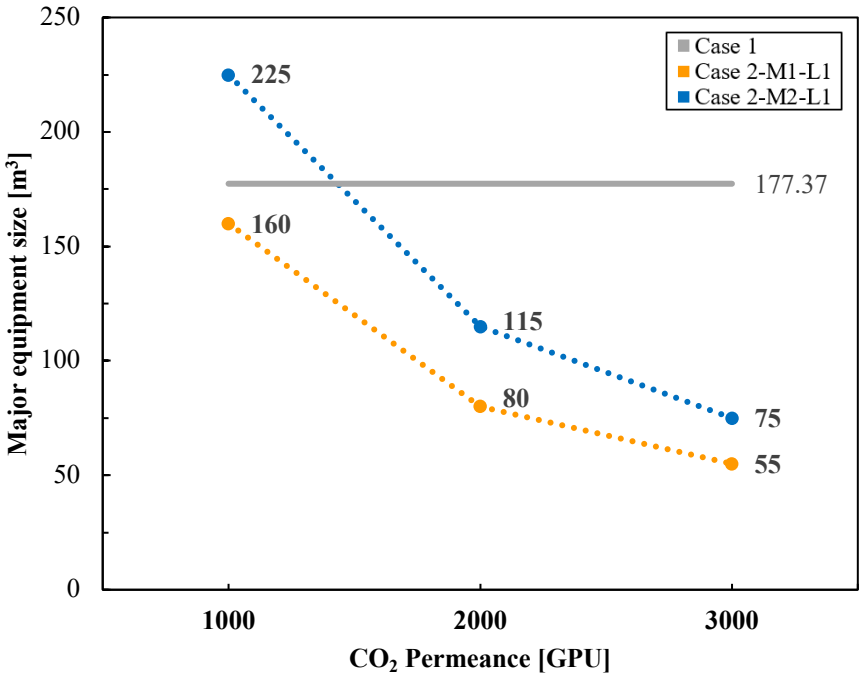

Figure 5. Major equipment size of Case 2 at selectivity 50 mixture

4.2 Case 3: membrane process with a ternary mixture (CO_2, N_2, and O_2)

The optimized results of Case 3 for the ternary mixture are shown in Table 12 and Figure 6 with CO_2/N_2 selectivity of 50, 100, and 150. A 100% recycling at R2 of M2-L1 and M2-L2 is

selected because the reject stream of the 2nd membrane stage had a higher CO_2 mole fraction than the exhaust gas. Recycling at R3 in design configurations of M1-L1 and M2-L1 is also selected because the single-stage liquefaction process (L1) cannot provide sufficiently low temperature to liquefy the required CO_2 compared to the ethane-propene cascade cycle (L2). This means that CO_2 in the inlet of the liquefaction process cannot be liquefied all at the temperature provided by the propene refrigeration cycle. Therefore, to liquefy the required CO_2, partial recycling at R3 of L1, which contains some amount of CO_2 is selected rather than an increase in stage cut of the membrane process, and this recycling decreases the energy consumption. For the ethane-propene cascade cycle, however, most of the CO_2 in the inlet of the liquefaction process can be liquefied because of the sufficiently low temperature provided by the L2. Therefore, the recycling at R3 of L2, which consists mostly of nitrogen and oxygen is not selected.

Table. 12. Simulation results of Case 3: ternary mixture

α	Configuration	θ_1 / θ_2 [%]	y_1/y_2 [mol%]	R1/R2/R3 [%]	P_4 [bar]	T_2 [°C]	SEC [GJ_e/t_{CO2}]		
							Capture	Liquefaction	Total
50	M1-L1	6.39 /-	20.31 /-	0/-/38	150	-69	1.591	3.708	5.517
	M1-L2	5.37 /-	21.58 /-	0/-/0	87	-99	1.494	2.467	3.984
	M2-L1	9.00 /24.31	19.55 /54.62	0/100/48	160	-53	2.999	1.467	4.835
	M2-L2	6.99 /32.14	20.71 /49.80	0/100/0	91	-89	2.639	1.262	3.975
100	M1-L1	5.40 /-	24.56 /-	0/-/36	164	-64	1.307	3.123	4.642
	M1-L2	4.41 /-	26.46 /-	0/-/0	91	-96	1.210	2.092	3.327
	M2-L1	6.70 /26.79	24.27 /67.69	0/100/37.08	140	-49	2.219	1.057	3.539
	M2-L2	5.42 /34.65	25.50 /61.04	0/100/0	67	-85	2.016	1.054	3.144
150	M1-L1	5.07 /-	26.51 /-	0/-/39	160	-63	1.207	2.998	4.418
	M1-L2	4.05 /-	28.87 /-	0/-/0	92	-95	1.104	1.948	3.077
	M2-L1	6.10 /25.04	26.90 /78.24	0/100/34	115	-47	2.016	0.864	3.074
	M2-L2	4.90 /32.99	28.09 /70.23	0/100/0	113	-85	1.810	0.962	2.818

Figure. 6 shows three major findings for the Case 3. The first one is a trade-off between the number of membrane stages and the energy consumption. When comparing M1-L1 with M2-L1, and M1-L2 with M2-L2, the two-stage membrane process (M2) had less energy consumption compared to the single-stage membrane process (M1) in all cases. When the CO_2 mole fraction captured from a membrane is low, the total flow rate after the capture process

going into the liquefaction process should increase to satisfy the required amount of CO_2 reduction. This makes the energy consumption in the liquefaction process higher. In addition, the required temperature for liquefaction should be lower when the CO_2 mole fraction is low, and this makes the energy consumption for the liquefaction process higher. The two-stage membrane process can produce higher CO_2 mole fraction; therefore, the energy consumption reduction in the liquefaction process is higher than the energy consumption increase due to the two-stage capture process. Additionally, when comparing M1-L1 and M2-L1 with M1-L2 and M2-L2, the energy consumption of the two-stage liquefaction (L2) configurations does not decrease significantly as the number of membrane stages increases. When the captured CO_2 mole fraction is low, the single-stage liquefaction process has to recycle through R3 point to satisfy the required amount of CO_2 reduction. While the two-stage liquefaction process provides a lower temperature for liquefying the CO_2 than the single-stage liquefaction. This means that the increase in the total flow rate for achieving the required LCO_2 is small even under low mole fraction conditions due to the decrease in the membrane stage.

The second trade-off is between the number of liquefaction stages and energy consumption. When comparing M1-L1 with M1-L2 and M2-L1 with M2-L2, two-stage liquefaction (L2) showed less energy consumption than single-stage liquefaction (L1). This was because the added ethane liquefaction process achieved a lower temperature than the single-stage liquefaction, which made it possible to decrease the flow rate after the capture process. In addition, two-stage liquefaction does not require recycling of the vapor stream to the inlet stream of liquefaction, so the energy consumed by the multi-stage compressors decreases.

The third observation is between the membrane selectivity and energy consumption; by increasing the CO_2/N_2 selectivity with a fixed O_2/N_2 selectivity, the energy consumption of the capture and liquefaction processes was gradually decreased. This was because the increasing

selectivity of the membrane produces high CO_2 mole fraction at the outlet stream of the membrane. This causes the total flow rate of the capture and liquefaction processes to decrease while being able to satisfy the required amount of CO_2 reduction, so that the energy consumption of both the capture and liquefaction processes decrease together. When a membrane with a selectivity of 150 was used, the M2-L2 process showed a lower energy consumption compared to the reference amine-based case, and M1-L2 and M2-L1 consumed a similar level of energy as the reference amine-based case.

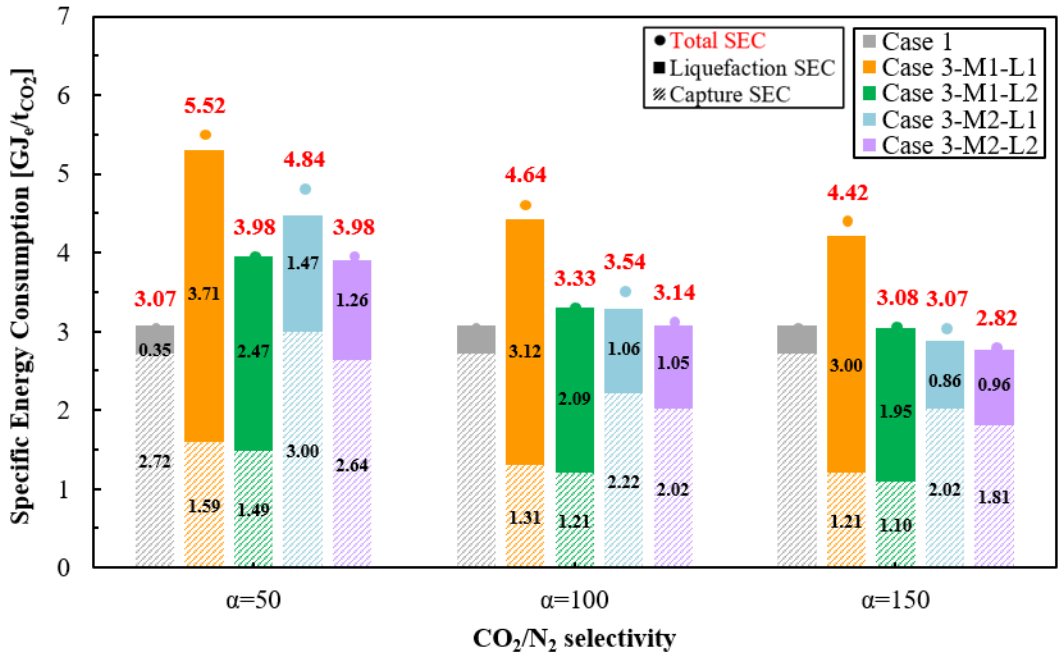

Figure 6. Total SEC and capture SEC of Case 3: membrane capture and liquefaction for the CO_2-N_2-O_2 ternary mixture

Table 13 shows the required membrane area and the number of membrane modules of Case 3 for estimating the major equipment size. Figure. 7 graphically shows the major equipment size of Case 3 according to the CO_2 permeance of 1000, 2000, and 3000 GPU with a fixed selectivity of 50. This indicated that the size of the membrane module drastically decreased

513 with increasing the CO_2 permeance. This means that effort to achieve a higher CO_2 permeance
514 is important to reduce the required membrane process size. All cases except M2-L1 with a CO_2
515 permeance of 1000 GPU showed a more compact size compared to that of the reference amine-
516 based case. When the CO_2 permeance was 2000 and 3000 GPU, the required sizes of the
517 membrane process were reduced by 28%–54% and 20%–37% of the Case 1, respectively.

518 Combining the results of energy and size, the number of stages for membrane and liquefaction
519 processes influenced the energy consumption because of the characteristics of the LNG-fueled
520 ship's exhaust gas which had low CO_2 mole fraction and high O_2 mole fraction. In addition,
521 the required membrane size was strongly affected by the variation in the CO_2 permeance.

522

523 Table. 13. Results of required membrane area of Case 3: ternary mixture

Permeance [GPU]	Configuration	Membrane area [m^2]	Number of membrane modules[*1]	Major equipment size[*2] (Modules volume) [m^3]
1000	M1-L1	57,216	23	115
	M1-L2	47,039	19	95
	M2-L1	92,986	38	190
	M2-L2	75,384	31	155
2000	M1-L1	28,608	12	60
	M1-L2	23,520	10	50
	M2-L1	46,493	19	95
	M2-L2	37,692	16	80
3000	M1-L1	19,072	8	40
	M1-L2	15,680	7	35
	M2-L1	30,996	13	65
	M2-L2	25,128	11	55

524 [*1] rounding up the number of membrane modules to the nearest one.
525 [*2] estimated by a 5 m^3 volume of MTR's membrane module.
526

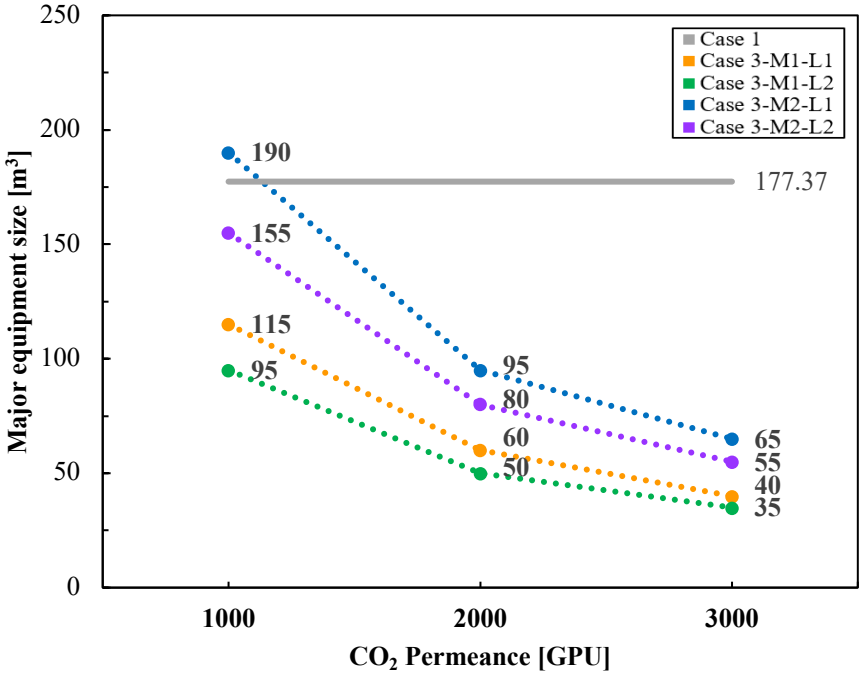

Figure 7. Major equipment size of Case 3 at selectivity 50

5. Conclusions

This study proposes an onboard membrane carbon capture and liquefaction system for LNG-fueled ships satisfying the IMO's 2050 target of EEDI 70% reduction, to overcome the large size problem of a conventional solvent-based CO_2 capture process. Because the exhaust gas from an LNG-fueled ship has the characteristic features of low CO_2 mole fraction and non-negligible oxygen content, a membrane process for a CO_2-N_2-O_2 ternary mixture was modeled and the low CO_2 mole fraction condition of an LNG-fueled ship was considered. Case studies were performed with various membrane stages, liquefaction stages, membrane selectivity, and permeance. The resulting energy consumption and membrane size were compared to the reference case, based on the amine-based capture process. The analyses revealed three major key points. First, a ternary mixture exhaust gas considering oxygen clearly showed a lower performance compared to the results of a binary mixture. This means that at least a ternary mixture exhaust gas should be considered for an LNG-fueled ship because the CO_2-N_2 binary mixture assumption of an exhaust gas could generate impractical results. Second, for a ternary mixture exhaust gas, the development of a CO_2/N_2 selectivity of 100 was required to achieve a similar level of energy consumption compared to the onboard amine-based capture system. Third, the membrane OCCS system was much smaller than the conventional amine-based process. With a membrane permeance of 1000, 2000, and 3000 GPU, the size of the membrane process can be only 54%, 28%, and 20% of amine-based capture process when comparing the major equipment size as volume, which indicated that the OCCS system using a membrane can be a good compact system for a ship. Consequently, these analyses indicated that the onboard membrane carbon capture and liquefaction system for LNG-fueled ships can be a practical and viable solution for the IMO's greenhouse gas targets for 2050, even under a ternary mixture condition of ship exhaust gas with low CO_2 mole fraction.

CRediT authorship contribution statement

Juyoung Oh: Conceptualization, Methodology, Visualization, Writing – Original Draft.

Rahul Anantharaman: Conceptualization, Writing – Review & Editing.

Umer Zahid: Validation, Writing – Review & Editing.

PyungSoo Lee: Methodology, Writing – Review & Editing, Supervision.

Youngsub Lim: Conceptualization, Methodology, Writing – Review & Editing, Supervision.

Declaration of competing interest

The authors declare that they have no known competing financial interests or personal relationships that could have appeared to influence the work reported in this paper.

Acknowledgements

This work was supported by the National Research Foundation of Korea (NRF) grant funded by the Korea government (MSIT) (No. 2021M3H7A102621612), and by the CCShip project funded by Wärtsilä Moss, Calix Limited, Klaveness, the Norwegian CCS Research Centre (NCCS), and the Norwegian Research Council through the MAROFF program (No. 320260). The Research Institute of Marine Systems Engineering at Seoul National University provided research facilities for this work.

References

[1] IMO, Fourth IMO GHG Study 2020 Full Report, 2021.

[2] IMO, Report of the marine environment protection committee on its 73th session, 2018.

[3] IMO, Report of the marine environment protection committee on its 74th session, 2019.

[4] IMO, Resolution MEPC.304(72); Initial IMO strategy on reduction of GHG emissions from ships, 2018.

[5] E.A. Bouman, E. Lindstad, A.I. Rialland, A.H. Strømman, State-of-the-art technologies, measures, and potential for reducing GHG emissions from shipping – A review, Transportation Research Part D: Transport and Environment. 52 (2017) 408–421. https://doi.org/10.1016/j.trd.2017.03.022.

[6] American Bureau of Shipping, Setting the course to low carbon shipping: 2030 outlook 2050 vision, 2019.

[7] J.P. Hong, Y.-S. Kim, H.-W. Shim, H.-J. Kang, Y. Kim, G.B. Kim, S. Cho, Study on a Fully Electrified Car Ferry Design Powered by Removable Battery Systems Considering Domestic Coastal Environment, Journal of Ocean Engineering and Technology. 35 (2021) 1–12. https://doi.org/10.26748/ksoe.2020.061.

[8] X. Luo, M. Wang, Study of solvent-based carbon capture for cargo ships through process modelling and simulation, Applied Energy. 195 (2017) 402–413. https://doi.org/10.1016/j.apenergy.2017.03.027.

[9] S. Lee, S. Yoo, H. Park, J. Ahn, D. Chang, Novel methodology for EEDI calculation considering onboard carbon capture and storage system, International Journal of Greenhouse Gas Control. 105 (2021) 103241. https://doi.org/10.1016/j.ijggc.2020.103241.

[10] M. Feenstra, J. Monteiro, J.T. van den Akker, M.R.M. Abu-Zahra, E. Gilling, E. Goetheer, Ship-based carbon capture onboard of diesel or LNG-fuelled ships, International Journal of Greenhouse Gas Control. 85 (2019) 1–10. https://doi.org/10.1016/j.ijggc.2019.03.008.

[11] P. Zhou, H. Wang, Carbon capture and storage - Solidification and storage of carbon dioxide captured on ships, Ocean Engineering. 91 (2014) 172–180. https://doi.org/10.1016/j.oceaneng.2014.09.006.

[12] J.T. van den Akker, Carbon capture onboard LNG-fueled vessels: A feasibility study, 2017. http://repository.tudelft.nl.

[13] S. Fang, Y. Xu, Z. Li, Z. Ding, L. Liu, H. Wang, Optimal Sizing of Shipboard Carbon Capture System for Maritime Greenhouse Emission Control, in: IEEE Transactions on Industry Applications, Institute of Electrical and Electronics Engineers Inc., 2019: pp. 5543–5553. https://doi.org/10.1109/TIA.2019.2934088.

[14] M. Kárászová, B. Zach, Z. Petrusová, V. Červenka, M. Bobák, M. Šyc, P. Izák, Post-

combustion carbon capture by membrane separation, Review, Separation and Purification Technology. 238 (2020). https://doi.org/10.1016/j.seppur.2019.116448.

[15] T. Merkel, J. Kniep, X. Wei, T. Carlisle, S. White, S. Pande, D. Fulton, R. Watson, T. Hoffman, B. Freeman, R. Baker, Pilot testing of a membrane system for post-combustion CO2 capture, Membrane Technology and Research, Incorporated, Newark, CA (United States), 2015.

[16] L. Zhao, E. Riensche, L. Blum, D. Stolten, Multi-stage gas separation membrane processes used in post-combustion capture: Energetic and economic analyses, Journal of Membrane Science. 359 (2010) 160–172. https://doi.org/10.1016/j.memsci.2010.02.003.

[17] A. Hussain, M.-B. Hägg, A feasibility study of CO 2 capture from flue gas by a facilitated transport membrane, Journal of Membrane Science. 359 (2010) 140–148. https://doi.org/10.1016/j.memsci.2009.11.035.

[18] T.C. Merkel, H. Lin, X. Wei, R. Baker, Power plant post-combustion carbon dioxide capture: An opportunity for membranes, Journal of Membrane Science. 359 (2010) 126–139. https://doi.org/10.1016/j.memsci.2009.10.041.

[19] K. Ramasubramanian, H. Verweij, W.S. Winston Ho, Membrane processes for carbon capture from coal-fired power plant flue gas: A modeling and cost study, Journal of Membrane Science. 421–422 (2012) 299–310. https://doi.org/10.1016/j.memsci.2012.07.029.

[20] J. Xu, Z. Wang, Z. Qiao, H. Wu, S. Dong, S. Zhao, J. Wang, Post-combustion CO2 capture with membrane process: Practical membrane performance and appropriate pressure, Journal of Membrane Science. 581 (2019) 195–213. https://doi.org/10.1016/j.memsci.2019.03.052.

[21] M. Micari, M. Dakhchoune, K. v. Agrawal, Techno-economic assessment of postcombustion carbon capture using high-performance nanoporous single-layer graphene membranes, Journal of Membrane Science. 624 (2021) 119103. https://doi.org/10.1016/j.memsci.2021.119103.

[22] C.J. Geankoplis, Transport processes and separation process principles:(includes unit operations), fourth ed., Prentice Hall Professional Technical Reference, 2003.

[23] W.P. Walawender, S.A. Stern, Analysis of Membrane Separation Parameters. II. Counter-current and Cocurrent Flow in a Single Permeation Stage, Separation Science. 7 (1972) 553–584. https://doi.org/10.1080/00372367208056054.

[24] S. Weller, W.A. Steiner, Separation of gases by fractional permeation through membranes, Journal of Applied Physics. 21 (1950) 279–283. https://doi.org/10.1063/1.1699653.

[25] A. Aspelund, M.J. Mølnvik, G. de Koeijer, Ship transport of CO2: Technical solutions and analysis of costs, energy utilization, exergy efficiency and CO2 emissions, Chemical Engineering Research and Design. 84 (2006) 847–855. https://doi.org/10.1205/cherd.5147.

664 [26] Y. Seo, H. You, S. Lee, C. Huh, D. Chang, Evaluation of CO2 liquefaction processes for
665 ship-based carbon capture and storage (CCS) in terms of life cycle cost (LCC)
666 considering availability, International Journal of Greenhouse Gas Control. 35 (2015) 1–
667 12. https://doi.org/10.1016/j.ijggc.2015.01.006.

668 [27] A. Aspelund, K. Jordal, Gas conditioning-The interface between CO2 capture and
669 transport, International Journal of Greenhouse Gas Control. 1 (2007) 343–354.
670 https://doi.org/10.1016/S1750-5836(07)00040-0.

671 [28] M. Ozaki, T. Ohsumi, CCS from multiple sources to offshore storage site complex via
672 ship transport, Energy Procedia. 4 (2011) 2992–2999.
673 https://doi.org/10.1016/j.egypro.2011.02.209.

674 [29] S. Decarre, J. Berthiaud, N. Butin, J.L. Guillaume-Combecave, CO2 maritime
675 transportation, International Journal of Greenhouse Gas Control. 4 (2010) 857–864.
676 https://doi.org/10.1016/j.ijggc.2010.05.005.

677 [30] U. Zahid, J. An, C.J. Lee, U. Lee, C. Han, Design and operation strategy of CO2 terminal,
678 Industrial and Engineering Chemistry Research. 54 (2015) 2353–2365.
679 https://doi.org/10.1021/ie503696x.

680 [31] Y. Seo, C. Huh, S. Lee, D. Chang, Comparison of CO2 liquefaction pressures for ship-
681 based carbon capture and storage (CCS) chain, International Journal of Greenhouse Gas
682 Control. 52 (2016) 1–12. https://doi.org/10.1016/j.ijggc.2016.06.011.

683 [32] A. Alabdulkarem, Y. Hwang, R. Radermacher, Development of CO2 liquefaction cycles
684 for CO2 sequestration, Applied Thermal Engineering. 33–34 (2012) 144–156.
685 https://doi.org/10.1016/j.applthermaleng.2011.09.027.

686 [33] S. Yang, U. Lee, Y. Lim, Y. Jeong, J. Kim, C. Lee, C. Han, Process design and cost
687 estimation of carbon dioxide compression and liquefaction for transportation, Korean
688 Chemical Engineering Research. 50 (2012) 988–993.
689 https://doi.org/10.9713/KCER.2012.50.6.988.

690 [34] G.N. Sakalis, G.J. Tzortzis, C.A. Frangopoulos, Intertemporal static and dynamic
691 optimization of synthesis, design, and operation of integrated energy systems of ships,
692 Energies. 12 (2019). https://doi.org/10.3390/en12050893.

693 [35] K. Khiraiya, P. v. Ramana, H. Panchal, K.K. Sadasivuni, M.H. Doranehgard, M. Khalid,
694 Diesel-fired boiler performance and emissions measurements using a combination of
695 diesel and palm biodiesel, Case Studies in Thermal Engineering. 27 (2021).
696 https://doi.org/10.1016/j.csite.2021.101324.

697 [36] L. Chao, L. Ke, W. Yongzhen, M. Zhitong, G. Yulie, The Effect Analysis of Thermal
698 Efficiency and Optimal Design for Boiler System, Energy Procedia. 105 (2017) 3045–
699 3050. https://doi.org/10.1016/j.egypro.2017.03.629.

700 [37] A.I. Papadopoulos, P. Seferlis, Process Systems and Materials for CO2 Capture, Wiley
701 Online Library, 2017.

702 [38] G. Dong, H. Li, V. Chen, Factors affect defect-free Matrimid® hollow fiber gas

703 separation performance in natural gas purification, Journal of Membrane Science. 353
704 (2010) 17–27. https://doi.org/10.1016/j.memsci.2010.02.012.

705 [39] M.A. Rodrigues, J. de S. Ribeiro, E. de S. Costa, J.L. de Miranda, H.C. Ferraz,
706 Nanostructured membranes containing UiO-66 (Zr) and MIL-101 (Cr) for O2/N2 and
707 CO2/N2 separation, Separation and Purification Technology. 192 (2018) 491–500.
708 https://doi.org/10.1016/j.seppur.2017.10.024.

709 [40] W. You, M. Chae, J. Park, Y. Lim, Potential Explosion Risk Comparison between SMR
710 and DMR Liquefaction Processes at Conceptual Design Stage of FLNG, Journal of
711 Ocean Engineering and Technology. 32 (2018) 95–105.
712 https://doi.org/10.26748/ksoe.2018.4.32.2.095.

713 [41] Wärtsilä, WSD80 3800 Container Feeder DATASHEET, (2016).
714 https://cdn.wartsila.com/docs/default-source/product-files/sd/merchant/feeder/wsd80-
715 3800-container-feeder-ship-design-o-data-sheet.pdf?sfvrsn=4871f445_12 (accessed
716 June 1, 2021).

717 [42] W.D. Seider, J.D. Seader, D.R. Lewin, S. Widagdo, Product and process design
718 principles: synthesis, analysis, and evaluation, John Wiley & Sons, 2009.

719 [43] Ship-technology, Onboard carbon capture: dream or reality?, (2013). https://www.ship-
720 technology.com/features/featureonboard-carbon-capture-dream-or-reality/ (accessed
721 June 28, 2021).

722